

Deformation, texture and fabric in soft clay soils

CM Wensrich,^{1,*} J Pineda,² V Luzin,³ L Suwal,² and EH Kisi¹

¹School of Engineering, The University of Newcastle, Australia

²ARC Center of Excellence for Geotechnical Science and Engineering, The University of Newcastle, Australia

³Australian Centre for Neutron Scattering, Australian Nuclear Science and Technology Organisation, Australia

(Dated: April 3, 2017)

Keywords: Soft soils; Clay; Texture; Fabric; Neutron diffraction

Highly compressible soft clay soils are commonly found on seabeds and estuarine deposits. These materials show complex mechanical behaviour that must be understood for effective design of foundations and geostructures for applications in; heavy-haul road pavements, offshore pipelines, oil and gas infrastructure, tunnel construction, excavations, and dams.

One of the more complicated aspects of these materials is the significant amount of anisotropy they can display. This anisotropy is directly linked to micro-structure; mechanical properties and permeability are sensitive to preferred orientations in the alignment of microscopic plate-like particles (see Figure 1a). The distribution of these orientations is often referred to as the *fabric* of the material. The evolution of clay fabric is directly related to the deformation and deposition history.

Modern constitutive models strive to capture these effects by modifying (rotating) the yield surface and flow rules (i.e. plastic potentials) in response to plastic strain (e.g. [1, 2]). This approach assumes a causal link between deformation, micro-structure and mechanical anisotropy, however the micro-mechanics of this are poorly understood.

The development of a proper understanding of the mechanisms behind anisotropy in clays relies on being able to accurately characterise the micro-structure of experimental samples. Since the pioneering work of Barden *et al.* [3, 4], Collins *et al.* [5] and Osipov *et al.* [6–8], various qualitative and quantitative techniques have been combined to examine the micro-structural properties of clays. Mercury Intrusion Porosimetry (MIP) and nitrogen adsorption tests ([9, 10][more here??](#); among others) can provide a measure of pore sizes and distributions, however fabric remains a challenge. Current practice usually involves microscopy, laboratory-based X-ray

sources (e.g. ...), and more recently synchrotron radiation [1]. These techniques can be limited to small samples or observations at or near the external surfaces which are not necessarily representative.

In this letter we present results from an experimental technique based on neutron diffraction that is able to provide a bulk characterisation of the fabric of representative experimental samples. This technique was utilised in two experiments focused on capturing the evolution of fabric within kaolin-clay samples as a function of composition and deformation. The letter will describe the details and outcomes of these experiments, however we begin by describing the experimental technique;

The plate-like nature of clay particles is directly related to their layered silicate crystal structure. As a consequence, the physical orientation of a clay particle corresponds perfectly with its crystallographic directions. From this perspective it is clear that the crystallographic *texture* of a clay sample directly provides information on the micro-structural *fabric*. Crystallographic texture is of prime concern in various areas of material science and a number of experimental techniques are available to provide such measurements. In particular, the penetrating nature of neutrons provides a method by which texture measurements can be made for bulk samples of the scale of centimeters depending on the material [11]. Figure 1a provides a typical experimental setup.

The approach relies upon the fact that the intensity of a diffracted beam depends directly on the volume of crystal grains that satisfy Bragg's law for a given orientation of the sample and instrument. With an incident beam of constant wavelength, the magnitude of a diffraction peak, I_{hkl} , as a function of sample orientation, $\hat{\mathbf{n}} = (\cos \psi \cos \phi, \cos \psi \sin \phi, \sin \psi)$, can be used to map-out the orientation density function for the corresponding lattice planes;

$$O_{hkl}(\hat{\mathbf{n}}) = \frac{I_{hkl}(\hat{\mathbf{n}})}{\langle I_{hkl} \rangle} \quad (1)$$

* Christopher.Wensrich@newcastle.edu.au

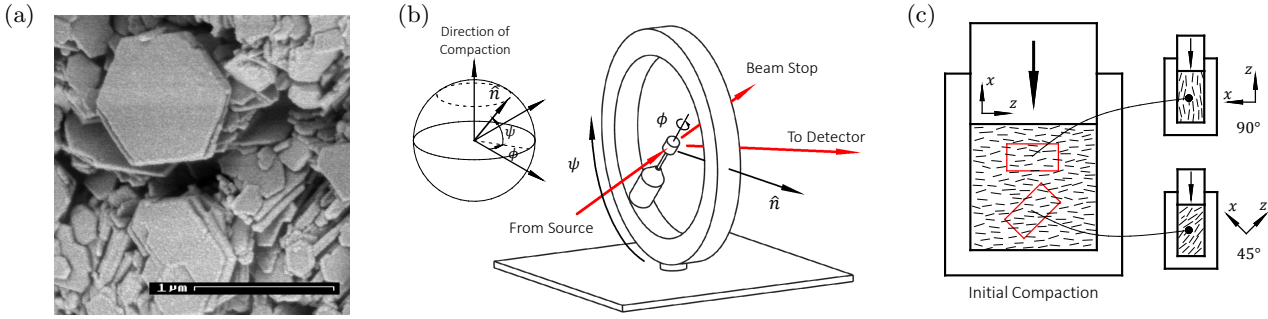


FIG. 1. (a) An SEM image of kaolin-clay showing discrete plate-like kaolin particles (**Note this one stolen from Web. Would be nice to have a more legit one**). (b) The geometry of a texture measurement using neutron diffraction. The intensity of the diffracted beam is proportional to the number of crystal grains with planes aligned in the direction \hat{n} . (c) Sample preparation for the second experiment involved two stages of deformation; an initial compaction to a reference condition followed by a second compaction at either 90° or 45° to the initial stage.

In the case of a kaolinite clay sample, the orientation density of various lattice planes (e.g. 0001 , 0002 etc.) directly provides the orientation density of platelets. Such a measurement directly defines the internal structure of a sample.

Orientation density can be used to calculate fabric tensors of the form [12];

$$F_{i_1 i_2 \dots i_r} = \frac{1}{2\pi} \int_0^{\frac{\pi}{2}} \int_0^{2\pi} O(\hat{n}) \hat{n}_{i_1} \hat{n}_{i_2} \dots \hat{n}_{i_r} \cos \psi d\phi d\psi, \quad (2)$$

where r is an arbitrary rank (note that $O(\hat{n}) = O(-\hat{n})$). A numerical version of this integral can easily be defined for measured experimental data.

Fabric tensors of this type can be used as a description of internal structure. In granular materials the fabric tensor usually refers to orientations of contacts, however the plate-like structure of clay particles implies equivalence in this case. Higher rank tensors can capture higher order variations in the structure, however in practice rank-2 is usually deemed sufficient. The trace of this tensor is unity, with random orientation implied by $F_{ij} = \frac{1}{3}\delta_{ij}$. In principal directions, diagonal components of the rank-2 fabric tensor refer to the relative size of principal diameters of an ellipsoidal orientation density function - higher rank tensors represent higher order spherical harmonics.

Our first experiment involved an examination of the evolution of fabric during compaction along with the effects of moisture on this process.

JP: Add sample prep info here

Texture in each sample was measured using the KOWARI diffractometer at the Australian Centre for Neutron Scattering (ACNS) within the Australian Nuclear Science and Technology Organisation (ANSTO). These measurements were based on the relative intensity of the (0002) diffraction peak from a monochromatic beam of neutrons of wavelength 2.8\AA . This relative intensity was measured over a $5^\circ \times 5^\circ$ regular grid over $0 < \phi < 360$ and $0 < \psi < 90$ using a standard 4-circle goniometer.

TABLE I. Sample properties for the first experiment

Sample Number	Dry Density [g/cc]	Moisture Content (by mass)
1	2.0	10%
2	1.75	10%
3	1.5	10%
4	1.25	10%
5	1.25	5%
6	1.25	20%
7	1.25	30%
8	1.25	35%

Hydrogen within hydroxyl groups in the sample create high background levels due to incoherent scattering. For this reason, relatively long sample times were necessary. The measurement of a complete orientation density required around 12 hours per clay sample.

Figure 2 shows the results of this experiment. 8 pole figures are shown arranged in the order indicated in the graph in the upper right corner. Each pole figure is a depiction of the orientation density function as viewed along the direction of compaction (notionally aligned with the third coordinate axis). Also shown in the upper right corner is the 33-component of the deviatoric part of the rank-2 fabric tensor,

$$F_{ij}^* = F_{ij} - \frac{1}{3}\delta_{ij}, \quad (3)$$

plotted as a function of either final density or moisture content. This component provides a measure of the degree of alignment of particles to the direction of compaction.

With the exception of the wettest sample, all of the pole figures indicate a purely *fibre* texture aligned with the direction of compaction to varying degrees. As expected, this indicates an alignment of platelets with their cleavage planes normal to the direction of compaction. The wettest sample shows a similar texture superimposed

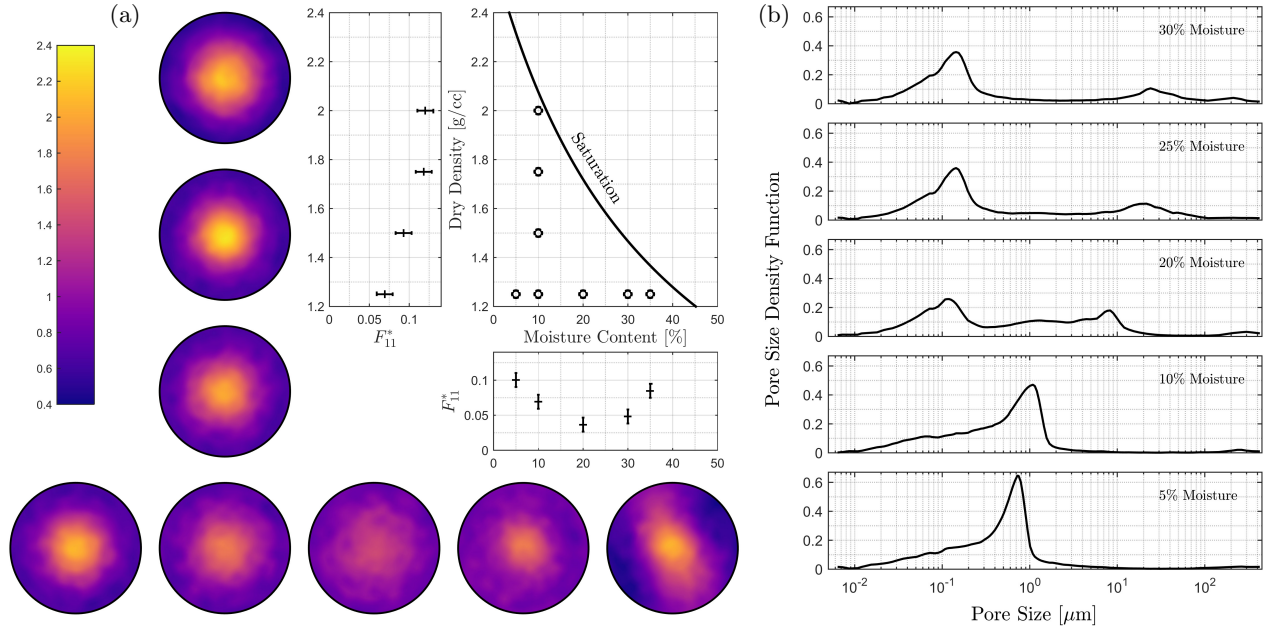


FIG. 2. (colour online) Results from the first experiment examining the evolution of fabric during compaction together with the effects of moisture content. (a) Pole figures show the three-dimensional orientation density of clay platelets as viewed in the direction of compaction. (b) Pore size distribution from MIP as a function of moisture content for a series of samples with 1.3g/cc dry density.

with a faint band of preferred directions. This is thought to be due to difficulties in the preparation of this sample associated with large agglomerates that were present prior to compaction. It is likely that the deformation of these agglomerates was not strictly axial.

Overall, the measurements show two interesting trends. First, the deviation of the fabric from the isotropic state of $F^* = 0$ increases with the level of compaction. This result is perhaps expected. Moisture seems to have a more varied effect; for the same final density, low and high levels of moisture lead to higher levels of alignment with a minimum in-between. **Need to add a story here including an overview of MIP testing and results**

Following the success of this experiment, a second experiment was devised to examine the relationship between the evolution of fabric and deformation for more complex loading paths. This experiment involved the preparation of clay samples through the following process;

A large initial sample was prepared by compacting kaolin at 10% moisture content within a 90mm diameter die to a density of 1.25g/cc. This compaction was performed in layers to reduce variation of properties in the axial direction. The initial state provided by this process corresponded to sample number 4 in the previous experiment. A number of smaller samples of 15mm diameter were then cut from this larger sample; 4 samples with their axis at 90° to the initial compaction direction, 4 at 45° . The initial length of each of these samples is

TABLE II. Sample properties for the second experiment. All samples had 10% moisture content and a final length of 10mm

Sample Number	Initial Length [mm]	Axial Strain	Density [g/cc]	Direction of Compaction
1	10	0	1.25	90°
2	12.2	0.18	1.52	90°
3	15.0	0.33	1.87	90°
4	16.6	0.41	2.12	90°
5	10	0	1.25	45°
6	12.2	0.18	1.52	45°
7	15.0	0.33	1.87	45°
8	16.6	0.41	2.12	45°

given in Table II. Each of these smaller samples were then compacted in their axial direction to a final length of 10mm. The final strain and density imposed by the second stage of compaction is also given in Table II. As before, each of these samples was freeze-dried to remove all moisture prior to texture analysis.

Using an identical instrument setup to the first experiment, texture measurements were performed on each of these 8 samples using the KOWARI diffractometer. Figure 3 shows the results of these measurements.

For each sample, a pole-figure depicting the orientation density is shown as viewed along the direction of the second stage of compaction. Colourmaps for these pole figures are individually normalised with the maximum

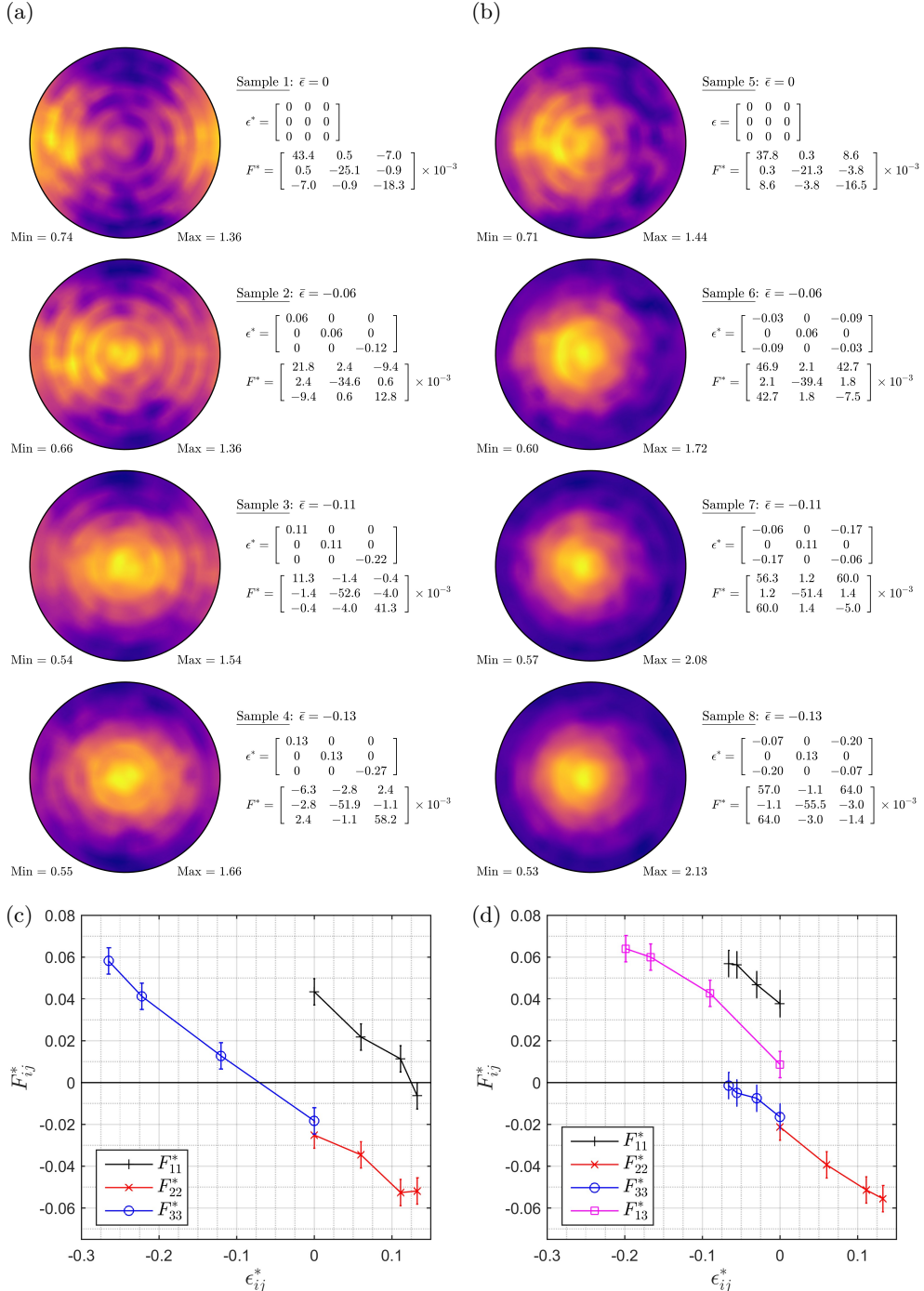


FIG. 3. (colour online) Evolution of structure within clay samples as a function of strain. With reference to Figure 1b, samples on the left are subject to strain at 90° to the initial direction of compaction, samples on the right are at 45° . Top - (a) and (b): pole figures show the three-dimensional orientation density as viewed in the direction of the second stage of compaction. Bottom - (c) and (d): individual components of the deviatoric fabric tensor as a function of the corresponding components of deviatoric strain.

and minimum values as indicated. Shown alongside is the corresponding deviatoric strain tensor ($\epsilon_{ij}^* = \epsilon_{ij} - \bar{\epsilon}\delta_{ij}$, where $\bar{\epsilon} = \frac{1}{3}\epsilon_{kk}$) and the deviatoric part of the rank-2 fabric tensor, both expressed in the original coordinate system as indicated in Figure 1c. At the bottom of Fig-

ure 3, individual components of the deviatoric fabric are plotted against corresponding components of deviatoric strain; components that do not significantly change are not shown. Error bars are based on the magnitude of components that are assumed to be zero.

Turning our attention first to samples 1 to 4 (i.e. 90° samples), we see that the second stage of compaction has produced a significant transformation in the orientation density function. The initial state shows preferred orientation in the x -direction in-line with the initial compaction process. As compressive strain is applied along the z -axis the preferred orientation migrates and then intensifies in-line with this direction. This effect can also be observed in the deviatoric fabric tensor which is approximately in principal directions over the whole loading path. The diagonal terms are initially dominated by the F_{11}^* component, which is offset by the F_{22}^* and F_{33}^* components in roughly equal amounts. As compressive strain is applied in the z -direction, the F_{33}^* component grows at the expense of the other two.

In terms of pole figures, samples 5 to 8 show similar behaviour. Over the second stage of compaction, the initial state of alignment transforms to align and intensify in the direction of compressive strain. However, in contrast to the 90° samples, the final state is subtly misaligned; the peak value of the orientation density is slightly to the left of centre. This is also observed in the fabric tensor which features a prominent F_{13}^* component in the final state. Note that this departure from principal directions is also present in the applied strain.

When viewed in relation to individual components of the strain tensor, the evolution of the fabric tensor becomes clear. From Figure 3 (c) and (d) we see that, within experimental error, components of the deviatoric fabric tensor change from their initial state at a constant rate with respect to the corresponding component of deviatoric strain. Of particular note; this rate of change appears consistent across all components - including those observed in the first experiment. Averaging across all

components provides the following simple relationship;

$$\frac{\partial F_{ij}^*}{\partial \epsilon_{ij}^*} = -0.28 \pm 0.01 \quad (4)$$

It should be made clear that this relationship was observed to hold over the range and direction of deformations examined in this experiment. Outside of this range, or in the case of other strain paths (e.g. direct shear or constant volume shear), the situation may vary. Nonetheless, the relationship would suggest that isotropic strain paths have no impact on fabric, and that principal directions of strain and fabric coincide if the initial state is random.

In conclusion, neutron based texture measurement techniques can provide a direct approach for assessing microstructure within clay samples. Through this approach we have been able to directly observe the distribution of the orientations of platelets in clay samples and uncover a simple relationship between deviatoric strain and the evolution of the fabric tensor. Given the direct link between mechanical properties and fabric, it is conceivable that this simple relationship could be integrated into an anisotropic constitutive model for this type of material. As opposed to current phenomenological approaches, this would allow the development of new constitutive models based directly on the micromechanics of these materials.

The authors would like to acknowledge support that made this work possible. In particular, access to the KOWARI diffractometer was made possible by the ACNS (formerly the Bragg Institute) within ANSTO through their user access program (proposals 4105 and 4308). Additional support during each experiment was also provided by the Australian Institute of Nuclear Science and Engineering (AINSE).

-
- [1] S. J. Wheeler, A. Nääätänen, M. Karstunen, and M. Lojander, Canadian Geotechnical Journal **40**, 403 (2003).
 - [2] G. Z. Voyatzis and C. R. Song, Journal of engineering mechanics **126**, 1012 (2000).
 - [3] L. Barden, in *Proceedings of International Symposium on Soil Structure*, Vol. 1 (Swedish Geotechnical Institute, 1973) pp. 21–26.
 - [4] L. Barden, A. McGown, and K. Collins, Engineering Geology **7**, 49 (1973).
 - [5] K. T. Collins and A. McGown, Geotechnique **24**, 223 (1974).
 - [6] V. Osipov and V. Sokolov, Bulletin of the International Association of Engineering Geology-Bulletin de l'Association Internationale de Géologie de l'Ingénieur **17**, 91 (1978).
 - [7] V. Osipov and V. Sokolov, Bulletin of Engineering Geology and the Environment **18**, 83 (1978).
 - [8] V. Osipov and V. Sokolov, Bulletin of the International Association of Engineering Geology-Bulletin de l'Association Internationale de Géologie de l'Ingénieur **18**, 73 (1978).
 - [9] P. Delage, Chinese Journal of Rock Mechanics and Engineering **25** (2006).
 - [10] E. Romero and P. H. Simms, in *Laboratory and Field Testing of Unsaturated Soils* (Springer, 2008) pp. 93–115.
 - [11] H.-R. Wenk, Reviews in Mineralogy and Geochemistry **63**, 399 (2006).
 - [12] K. Ken-Ichi, International Journal of Engineering Science **22**, 149 (1984).